nature communications

Article

https://doi.org/10.1038/s41467-026-68594-y

Homogenization of Northern Belgian landscapes through centuries of reclamation, agricultural transition, and urbanization

Received: 27 November 2024

Accepted: 8 January 2026

Published online: 21 January 2026

Check for updates

Luc De Keersmaeker[1] ✉, Pieter Roggemans[2], Lien Poelmans[3], Frederik Priem[3], Stijn Taillir[4], Toon Petermans[4] & Jo Van Valckenborgh[4]

We quantify historical land-use with deep learning image segmentation (GeoAI), applied to tiled historical maps, and identify 3 successive drivers of long-term (1774-2022) landscape transformation in northern Belgium (13,800 km^2). Between 1774 and 1873, reclamation halved the area of long-established forests, heathland, marshland, and the intertidal zone, i.e. natural and semi-natural land-use. Agricultural transition by globalization was the main driver in the next time interval (1873-1969), as the area of grassland and orchard doubled at the expense of arable land. Urbanization marked the last time interval (1969-2022) and reduced agricultural land-use. The reclamation of fertile soils first increased the association of land-use with soil, but after 1873 this association progressively weakened and land-use interspersed. Here, we demonstrate that GeoAI can generate high-resolution area-wide historical land-use maps to study the extent and rate of landscape transformation, which in our case resulted in the homogenization of previously distinct landscapes.

Historical land-use and consecutive land-use changes through time, along with the spatial context in which these occurred, determine to a high degree the characteristics and functioning of present-day landscapes. For instance, the decline and fragmentation of previously extensive land-use patches explain biodiversity hosted by present-day landscapes[1]. By identifying and quantifying the legacy effects of past land-use, landscape managers can develop strategies for biodiversity conservation and ecosystem restoration[2]. Similarly, threatened cultural landscapes with heritage values can be identified to set priorities for conservation[3]. Past land-use can also explain the quality and the evolution over time of the ecosystem services landscapes can provide[4].

Mapping of historical land-use and its changes is highly relevant for research at the interfaces of ecology, geography, and history[1–6] However, the availability and quality of historical sources often restrict data collection and analyses[7]. Land-use changes over the past decades can be quantified and evaluated using remote sensing data, even on a global scale[8]. For studies that cover a longer time span, e.g., centuries, reconstructions of historical land-use rely on databases of historical documents (e.g., census data), historical maps or pictures, natural archives (e.g., pollen or charcoal), or multiple-source data that can feed reconstruction models[5,6,9].

Historical topographic maps represent invaluable archives offering detailed insights into landscape configurations and land-use dynamics of past centuries[10]. Until recently, manual digitizing to some extent was necessary to create area-wide maps of historical land-use. Studies that applied this labor-intensive methodology focused on relatively small areas[11]. Machine learning and deep learning image classification techniques developed for remote sensing, also named

[1]Research Institute for Nature and Forest, Herman Teirlinckgebouw, Brussels, Belgium. [2]Agency for Agriculture and Fisheries, Brussels, Belgium. [3]Flemish Institute for Technological Research (VITO NV), Mol, Belgium. [4]Digital Flanders Agency, Herman Teirlinckgebouw, Brussels, Belgium.
✉e-mail: luc.dekeersmaeker@inbo.be

GeoAI, opened up new possibilities for the automated or semi-automated extraction of digital spatial information from historical maps, which are analog by origin[12].

For this work, it is a prerequisite to use high-quality scans of historical maps that are accurately georeferenced. The assemblage of map tiles expands the spatial extent of the area to which GeoAI can be applied (see e.g., ref. 13). But even then, the study of land-use changes based on historical maps is conditioned by map qualities, i.e., the native scale, the map extent, the geometric accuracy, and the quality of the drawing and the legend[10]. Furthermore, shifting semantics of historical maps over time can complicate the analysis of land-use changes[14].

Recent studies of land-use changes that applied GeoAI to historical maps demonstrate a tradeoff between the spatial extent, the native scale, and the number of discerned land-use classes (Table 1). Studies that cover an area of at least 10,000 km^2 in France[15], Great Britain[16] and Sweden[17], included only 1 historical map with a native scale less than 1:50,000 and extracted no more than 5 land-use classes. By contrast, similar studies in Denmark[18], Finland[19] and Ireland[20] used maps with higher native scales of at least 1:20,000 and extracted up to 10 land-use classes, but covered a much smaller area (Table 1).

In this work, we apply deep learning GeoAI to 3 tiled historical maps for area-wide semantic segmentation of land-use in northern Belgium, on the west side of the North European Plain (Fig. 1a, b). The quality of the 3 selected map series enables us to discern 9 common land-use classes with a high spatial resolution, using a 10 × 10 m grid, and for a relatively large area of 13,800 km^2 (Table 1). The selected maps were drawn at pivotal times in the history of Western Europe. The oldest map series, finished in 1774, is a baseline depicting the landscape at the end of the Ancien Régime, just before it was impacted by industrialization and the French rule[21]. The second map series was finished in 1873, when globalization triggered an agricultural transition[22,23]. The third map series, published in 1969, depicts northern Belgium in the first decades after World War II, an era of fast modernization and increasing prosperity. The resulting high-resolution and area-wide historical land-use maps, complemented with a present-day land-use map, provide 4 time slices that span almost 250 years. Given these characteristics, our study functions as a proof of concept for applying GeoAI to historical maps, to quantify long-term landscape transformation. We hypothesize that in our study area—characterized by a soil zonation typical of the North European Plain (Fig. 1c, d)—the association between land use and soil has weakened over time[24], leading to a homogenization of landscapes[25].

Results

Land-use change

Land-use on the 1774, 1873, and 1969 maps was detected with overall accuracies of 94%, 91% and 93%, respectively (Supplementary Tables S1–3). High values for both the user's and producer's accuracies of land-use classes with high area proportions (Table 2), attribute to the high overall accuracies. Whereas user's accuracies are consistently high, producer's accuracies are relatively low, indicating area underestimations by the maps, for orchard (1774, 1873), water (1774), built-up & garden (1873), the intertidal zone (1969) and freshwater marsh (1969) (Supplementary Tables S1–3). The 1774 and 1873 maps, respectively, manual drawings and color lithographs, do not have a uniform display. In particular small land-use patches resembling the surroundings, e.g., orchard adjacent to forest, are affected by segmentations errors. The 1969 map has a uniform coloring and symbol palette, but the complex symbology of the intertidal zone and marshes explains the misclassifications.

Whereas the area of surface water was always between 2% and 3% of northern Belgium, area proportions of all other land-use classes changed between 1774 and 2022 (Table 2). The area of heathland & dune occupied an estimated 11.8% of the study area in 1774, mostly in the Northeast (Fig. 2), but was reduced by half in 1873. This land-use continued to decline after 1873, to 1.4% in 2022. Freshwater marsh (0.8%) and the intertidal zone (0.5%) covered much smaller areas in 1774, but were also prone to a strong decline between 1774 and 1873. The grassland area was stable (11.5–12.4%) in the first century and marked river valleys and polders on the 1774 and 1873 maps (Fig. 2). It doubled in the next time interval, up to 26.9% in 1969, but this strong increase was followed by a decline to 21.8% in 2022. Arable land had the highest area proportion until 1969, but was surpassed by built-up & garden in 2022. Whereas more than 50% of northern Belgium was used as arable land in the eighteenth and nineteenth centuries, this proportion declined to 36.4% in 1969 and 27.3% in 2022. The total forest area did not change much between 1774 and 1969 (9.3–10.2%) and slightly increased to 12.7% in 2022. The area used for orchards amounted to 4.7% in 1969, but declined to 1.8% in 2022. Built-up & garden continued to increase from 6.4% in 1774 to 29.3% in 2022 (Table 2 and Fig. 2).

Association of land-use with soil

The V-score that represents the overall association of nine land-use classes with seven soil groups, including not specified soils, first increased (1774–1873), but declined after 1873 to values below that of 1774 (Fig. 3). This trend was mostly explained by the homogeneity of land-use in soil, whereas the completeness only declined in the last time interval (Fig. 3).

The increase of the homogeneity of land-use in soil in the first time interval indicates that soil groups were more composed of the same land-use class in 1873 than a century before. In 1774, arable land occupied more than 50% of sandy loam, silt loam, and polder soils that cover 46% of northern Belgium (Fig. 1), and this dominance further increased between 1774 and 1873 (Fig. 4a2–a4). The increase of arable land (Fig. 4a6) and grassland (Fig. 4e6) on alluvial soil, and the increase of grassland on wet & organic soil (Fig. 4e5) also contributed to the homogeneity increase, but both soils only cover 12% of northern Belgium (Fig. 1). On sand soil, covering 27% of northern Belgium (Fig. 1), there are antagonistic effects of shifting land-use proportions on the homogeneity (Fig. 4a1–f1).

The decline of homogeneity in the second time interval (1873–1969) is explained by the decline of arable land on sand, sandy loam, silt loam, and polder soils (Fig. 4a1–a4), which cover together 73% of northern Belgium. This decline of arable land is primarily counterbalanced by the increase of grassland (Fig. 4e1–e4). The increase of orchard on silt loam soil (Fig. 4h3) and the increase of forest on wet & organic soil (Fig. 4c5), where grassland decreased (Fig. 4e5), also contributed to the homogeneity decline.

The increase of built-up & garden on all except not specified soils (Fig. 4b1–b6) explains the further decline of homogeneity in the last time interval (1969–2022). The increase of built-up & garden is

Table 1 | Comparison of recent land-use change studies that applied GeoAI (machine and deep learning) techniques to historical maps, for the covered area, the native scale of the oldest map, the studied time span, the included number of time slices, and the extracted number of land-use (LU) classes

Country	Area (km^2)	Native Scale	Time span (years)	Time slices	LU classes	Reference
Belgium	13,800	1:11,520	248	4	9	This study
Denmark	595	1:20,000	138	2	10	[18]
Finland	900	1:20,000	57	4	5	[19]
France	100,000	1:86,400	238	2	4	[15]
Great Britain	209,331	1:63,360	75	2	5	[16]
Ireland	3025	1:10,565	172	2	2	[20]
Sweden	170,763	1:100,000	100	2	1	[17]

https://doi.org/10.1038/s41467-026-68594-y

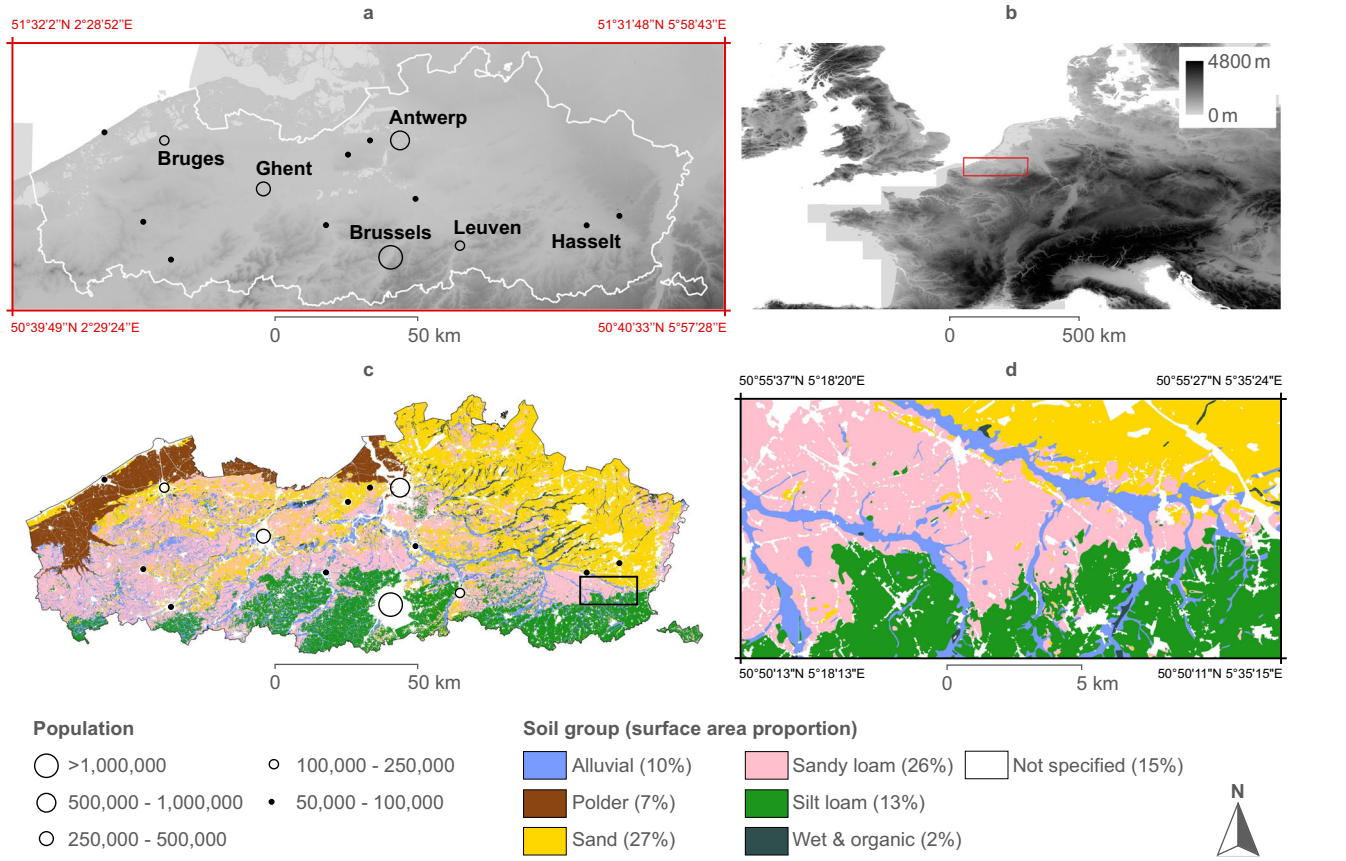

Fig. 1 | Northern Belgium is a densely populated region located at the west side of the North European Plain with a characteristic silt loam to sand soil zonation. Northern Belgium is a flat or undulating region with an altitude below 300 m above North sea level (**a**), located within the red box depicted at the west side of the North European Plain, as shown by the EuroDEM digital elevation model[70] (**b**). Soils of northern Belgium, classified in seven groups[59], display a north-south zonation from sand over sandy loam to silt loam soils, intersected by river valleys marked by alluvial and wet & organic soils and with polder soil along the coast and the Scheldt estuary (**c**). Names of the provincial and country capitals are labeled (**a**) and symbols (**a**, **c**) mark municipalities with a population of at least 50,000 inhabitants[63]. The area of the black box (**c**) is displayed enlarged (**d**). The EuroDEM dataset used in (**a**) and (**b**) includes Intellectual Property from European National Mapping and Cadastral Authorities and is licensed on behalf of these by EuroGeographics. The original dataset is available for free at https://www.mapsforeurope.org. Terms of the licence available at https://www.mapsforeurope.org/licence. All attribution statements can be found here. **c** and **d** are adapted from: De Keersmaeker, L. et al. Application of the Ancient Forest Concept to Potential Natural Vegetation Mapping in Flanders, A Strongly Altered Landscape in Northern Belgium. Folia Geobotanica 48, 137–162 (2013), Springer Nature, reproduced with permission from SNCSC.

Table 2 | Area proportions (%) of nine land-use classes at four time slices in northern Belgium

Land-use class	1774		1873		1969		2022
	Area (%)	CI (%)	Area (%)	CI (%)	Area (%)	CI (%)	Area (%)
Arable land	51.3	1.9	55.2	3.2	36.4	1.4	27.3
Built-up & garden	6.4	1.2	11.5	2.8	16.6	1.2	29.3
Forest	10.2	0.5	9.3	0.4	9.5	0.2	12.7
Freshwater marsh	0.8	0.1	0.3	0.1	0.2	0.1	0.3
Grassland	11.5	0.9	12.4	0.7	26.9	1.0	21.8
Heathland & dune	11.8	0.3	6.4	1.2	3.1	0.3	1.4
Intertidal zone	0.5	0.1	0.3	0.0	0.4	0.3	0.1
Orchard	3.6	1.6	2.1	1.2	4.7	0.9	1.8
Water	2.8	0.7	2.4	0.4	2.2	0.6	2.4
Mapped area	99.0		99.9		100.0		97.1
Not specified	1.0		0.1		0.0		2.9

The 1774, 1873, and 1969 area proportions are estimates with 95% confidence intervals CI (%) based on the validation of the GeoAI segmentation (Supplementary Tables S1–S3, respectively).

counterbalanced by the decline of arable land on sand, sandy loam, silt loam, and polder soil (Fig. 4a1–a4). Grassland declined where it was dominant in 1969 (Fig. 4e5, e6), by contrast forest increased on these wet & organic and alluvial soils (Fig. 4c5, c6).

Not specified soils contain areas that were disturbed or not mapped at the time the soil map was drawn (1947–1971). Inherently, the proportion of not specified soils occupied by built-up & garden increased over time (Fig. 4b7), counteracting the decline of

https://doi.org/10.1038/s41467-026-68594-y

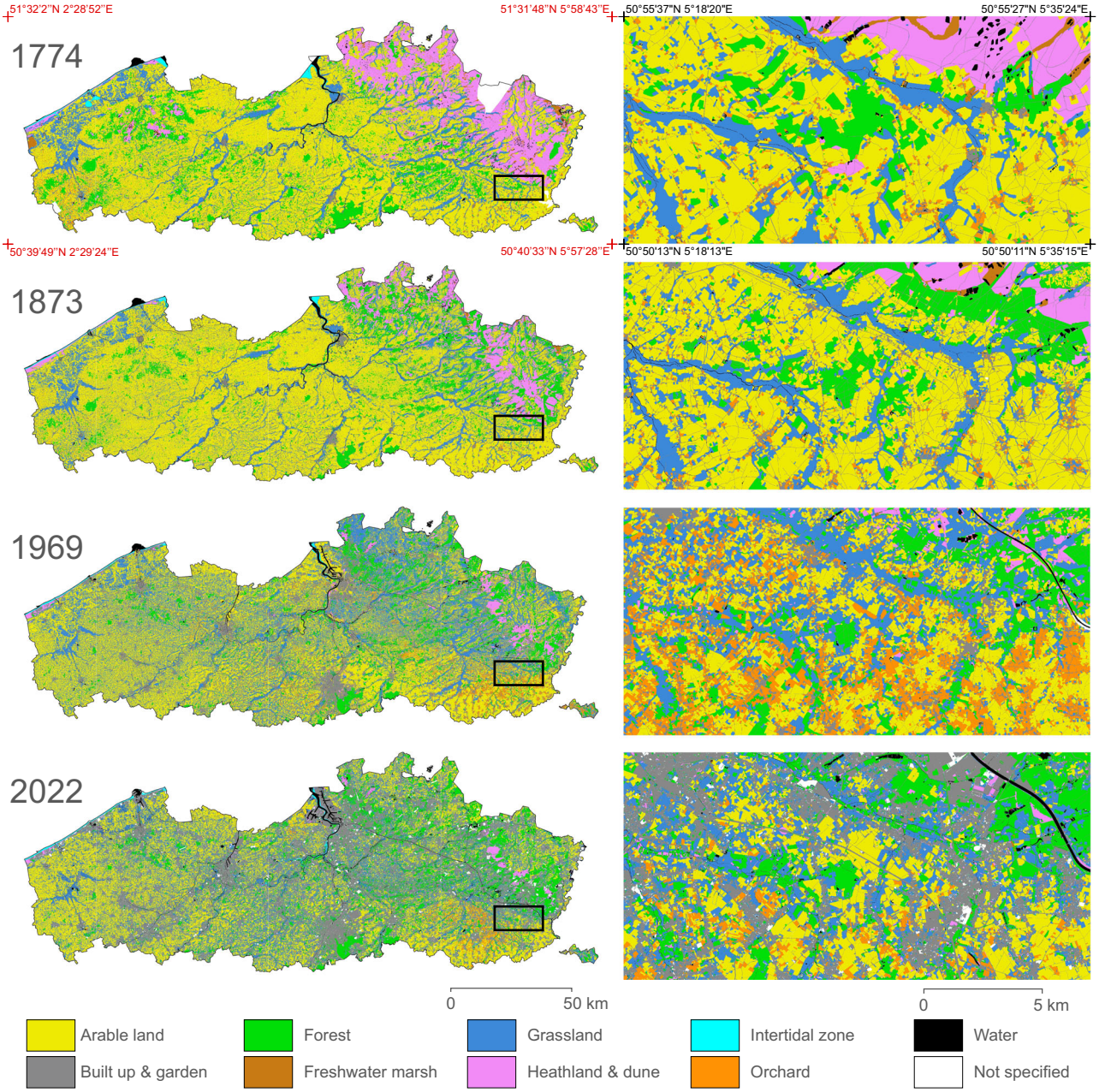

Fig. 2 | Land-use change in northern Belgium between 1774 and 2022. Land-use in northern Belgium (red box in Fig. 1a) is mapped in nine classes and not specified land-use, using a grid with 10 × 10 m resolution for spatial analyses. The area of the black box at the transition of silt loam to sand soils (Fig. 1d) is enlarged at the right side.

homogeneity. Conversely, the proportion of not specified soil in built-up & garden declined after 1969 (Fig. 4b7). As the soil map was mostly completed at that time, built-up & garden increased on other than not specified soils in the last time interval (Fig. 4b1–b6). This contributed to the decline of completeness, indicating that land-use became less concentrated in a single soil group.

Autocorrelation and interspersion

An increase or decline of spatial autocorrelation, expressed by global Moran's I, indicates that a land-use class respectively became less or more fragmented over time. The increased fragmentation of arable land (Fig. 5a), heathland & dune (Fig. 5e), the intertidal zone (Fig. 5f), and marshes (Fig. 5g) accompanied the area decline of these land-use classes. Conversely, fragmentation of built-up & garden was reduced (Fig. 5b) as the area increased. Fragmentation and area of grassland and orchard altered in a deviant way from the aforementioned land-use classes. Although the grassland area doubled between 1774 and 2022 (Table 2), its dispersed increase on soils where it was previously scarce in the second time interval (Fig. 4e1–e3), followed by a decline where it was dominant in the last interval (Fig. 4e5, e6), increased fragmentation over time. The fragmentation of orchard was lower in 2022 than before (Fig. 5h), although the area declined in the last time interval (Table 2). The contraction of this land-use to silt loam soils (Fig. 4h3) in the Southeast (Fig. 2) is explanatory.

A complementary metric to evaluate the change of the landscape texture is the interspersion level, which refers to the spatial intermixing of different patch types, land-use classes in this case, without explicit reference to the fragmentation level that we quantify by means of global Moran's *I*. In 1774 and 1873, the interspersion level was less than 50% for approximately two thirds of northern Belgium (Fig. 6). River valleys, where several land-use classes converged, were accentuated by high interspersion levels, whereas vast areas of arable land,

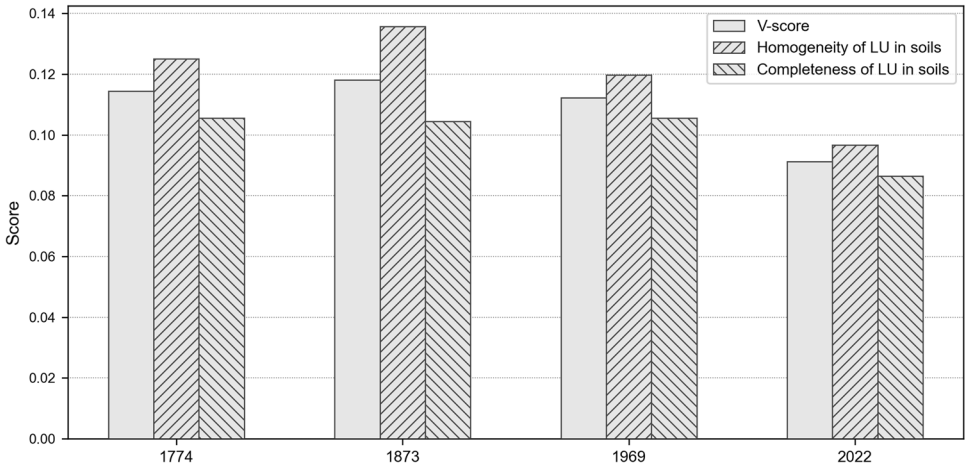

Fig. 3 | The change of the association between nine land-use (LU) classes and seven soil groups (soils) in northern Belgium, from 1774 to 2022. The homogeneity of land-use in soils measures how much of a soil group is composed of the same land-use class. The completeness measures how much of a land-use class is located within the same soil group. The V-score or global association simultaneously assesses homogeneity and completeness. The measures are calculated on 10 × 10 m grids of the soil map (Fig. 1c) and land-use maps at four time slices (Fig. 2).

heathland & dune, and forest displayed the lowest interspersion levels (compare Fig. 2 and Fig. 7). Interspersion increased between 1774 and 1873 in the Northeast (Fig. 7), as a result of forest and arable land intruding the heathland & dune area (Fig. 7). Between 1873 and 1969 the interspersion of land-use classes increased sharply (Fig. 6) and masked the hydrological structure (Fig. 7), as a result of the dispersed increase of grassland and built-up & garden (compare Fig. 2 and Fig. 7). Expanding cities, e.g. Brussels, Antwerp, Ghent and Bruges (Fig. 1a), are islands of homogeneous land-use with little interspersion in 1969 and 2022 (compare Fig. 2 and Fig. 7).

Discussion

The 1774 map was finished before socioeconomic changes, following the French invasion in 1795, and industrialization transformed the landscape[21]. But already in the second half of the eighteenth century, there was a strong population growth in northern Belgium[26]. At that time, agricultural reclamation was the primary response to population growth, causing the cropland area in European countries to peak around 1900[27]. The land-use changes in northern Belgium in the first time interval support this assumption, as heathland & dune, marshes, long-established forests, and the intertidal zone, i.e., natural and semi-natural land-use, declined and arable land and grassland expanded.

Heathland & dune and marshes, mostly located on sand soil, covered more than 12% of northern Belgium in 1774. These were used as common land for pasturing, cutting of peat, digging of loam, and wood gathering. In Northwestern Europe, the degradation of common land-use geared up in the last decades of the eighteenth century[28]. Within a century, the area of heathland & dune in northern Belgium was approximately reduced by half, and the decline continued up to 2022. The changes of land-use proportions on sand soil (Fig. 4a1, c1, f1) suggest that reclamation to arable land and forest plantation, respectively, accounted for one-third and two-thirds of this area loss. In northern Belgium, marshes and the intertidal area were already reduced by 50% between 1774 and 1873, whereas the worldwide loss of wetlands is assumed to have largely taken place in the twentieth century[29]. Our findings could confirm that the conversion of marshes to wet grasslands, also classified as wetlands, preceded the desiccation and conversion of the latter[30].

Although fossil pit coal fueled the early industrialization of Belgium from 1750 onward[31], forests remained important for energy supply at least until the first decades of the nineteenth century[32]. However, in the aftermath of the French Revolution, forests of the clergy and aristocracy were confiscated, privatized, and converted to farmland[32]. In many parts of Europe, the forest area was at a minimum in the nineteenth century as a result of agricultural expansion[33]. The already low total forest area in northern Belgium did not change much between 1774 and 1873, as the conversion of heathland & dune and marshes to plantation forests with coniferous trees[32] compensated for the loss of 50% of the forests on sandy loam, silt loam, and alluvial soils. These low net forest area changes thus conceal the erosion of long-established ancient forests with a high naturalness[34].

European agriculture was challenged by globalization after 1870, in particular by the cheap import of overseas cereals[22,23]. This triggered a strong increase in livestock production at the end of the nineteenth century and even more in the twentieth century[35–37]. In England[38] and the Netherlands[24] globalization caused a shifted from cropland to pasture, and our study quantifies that the grassland area in northern Belgium doubled between 1873 and 1969, as a result of this agricultural transition. By contrast, the increased focus on livestock production did not inflict such land-use change in Germany[39], Spain[40], Denmark[41] and Czech Republic[42]. Belgian agriculture not only shifted to livestock production, but also to horticulture and fruit production[23]. The area of orchards increased between 1873 and 1969, and concentrated on silt loam soils in the Southeast of our study area, whereas dispersed farm-based orchards disappeared[11].

The built-up & garden area increased from 6.4% in 1774 to 29.3% in 2022, which is more or less proportional to the population growth in that time interval. Population growth exceeded the area increase of built-up & garden between 1774 and 1969, first by rural proto-industrialization[26], later by urban transition, i.e., the transformation from a rural to an urban society during industrialization[43]. If we only consider the last time period (1969–2022), the area increase of built-up & garden (+76%) far exceeded population growth (+23%). A decline of population density in built-up areas, e.g., as a result of low-density residential housing, is an indicator of urban sprawl[44]. Our area-wide results confirm previous assessments of urban sprawl based on indirect population data at the level of municipalities[45] and case studies[46]. In northern Belgium, which is densely populated and urbanized since the Middle Ages[47], urban sprawl manifests itself as ribbon development guided by the historical pattern of villages, roads, and dikes[48]. As a result, this region is a hotspot of urbanization in recent decades[49]. The increase of built-up & garden after 1969 was proportional on all soil groups, so polder, wet & organic, and alluvial soils were not avoided. This is a confirmation of case studies of river valleys[11] and the assessment that newly established settlements in Belgium (1985–2015) are evenly distributed over flooding risk categories[50].

https://doi.org/10.1038/s41467-026-68594-y

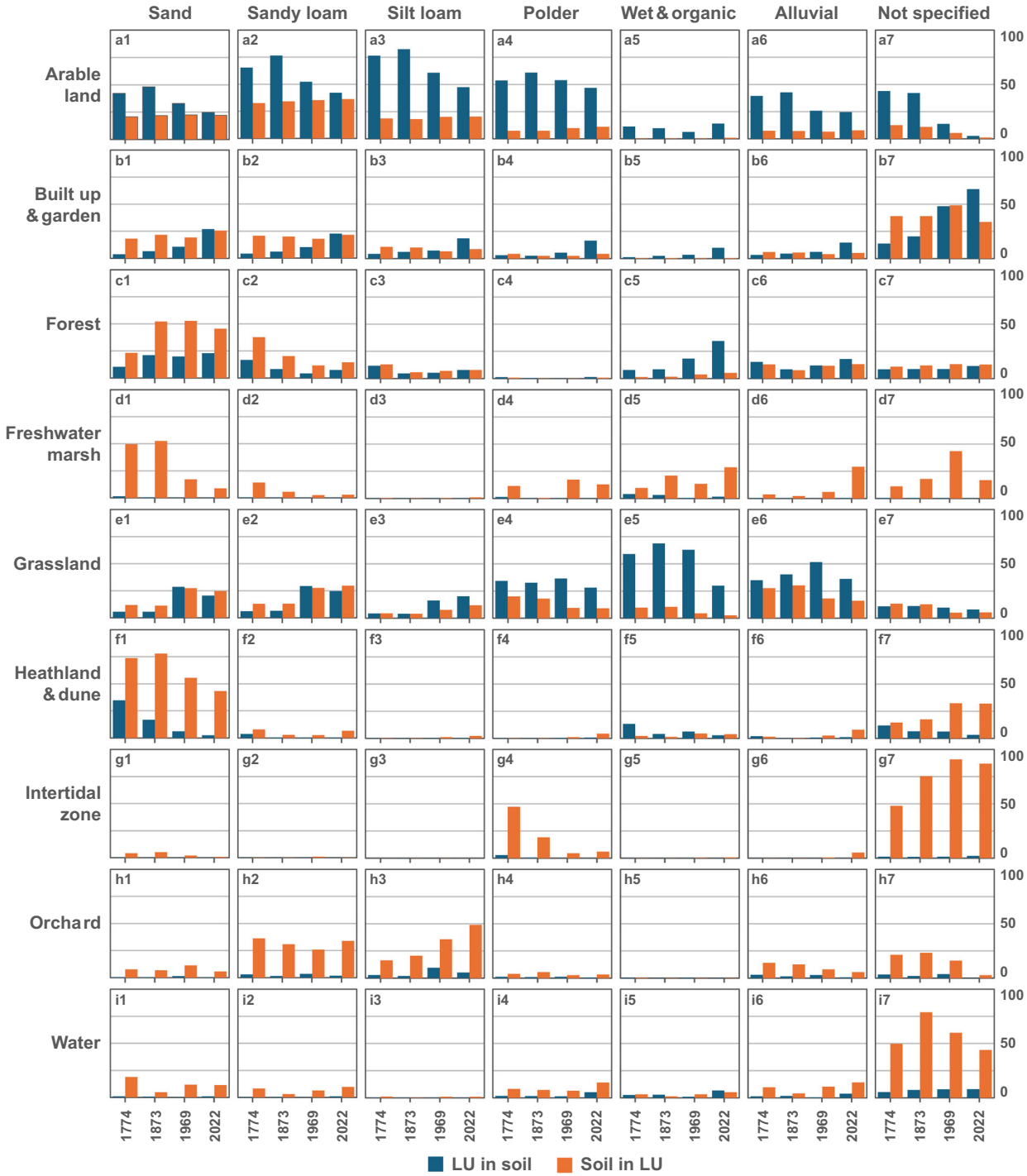

Fig. 4 | The change of proportions (%) of land-use classes in soil groups and soil groups in land-use classes in northern Belgium, between 1774 and 2022. Land-use classes are ordered in rows: arable land (**a1**–**a7**), built-up & garden (**b1**–**b7**), forest (**c1**–**c7**), freshwater marsh (**d1**–**d7**), grassland (**e1**–**e7**), heathland & dune (**f1**–**f7**), intertidal zone (**g1**–**g7**), orchard (**h1**–**h7**), and water (**i1**–**i7**). Soil groups are ordered in columns: sand (**a1**–**i1**), sandy loam (**a2**–**i2**), silt loam (**a3**–**i3**), polder (**a4**–**i4**), wet & organic (**a5**–**i5**), alluvial (**a6**–**i6**), and not specified soil (**a7**–**i7**). The sum of nine land-use classes in a soil group (LU in soil), as well as the sum of seven soil groups in a land-use class (Soil in LU), both equal 100% (*y*-axis).

The three drivers of land-use change, being land reclamation, agricultural transition, and urbanization followed each other in time. As a result of land reclamation, the overall association between land-use and soil patterns in northern Belgium first increased. In a similar way, by conversion of forest to arable land, the natural potential of fertile sites was further unleashed in nineteenth century Germany[51] and Poland[52]. As opposed to these areas in Germany and Poland that are still rural, the association between site conditions and land-use progressively weakened in northern Belgium after 1873. A similar trend occurred in the Netherlands between 1900 and 1990, also with an increase of grassland on a wide range of soil groups favoring this trend and a concentration of forest on sand soil opposing it[24]. A comparison of regional differences in Estonia revealed that the increase of high-intensity land-use weakened the association with soil patterns and homogenized landscapes[25].

https://doi.org/10.1038/s41467-026-68594-y

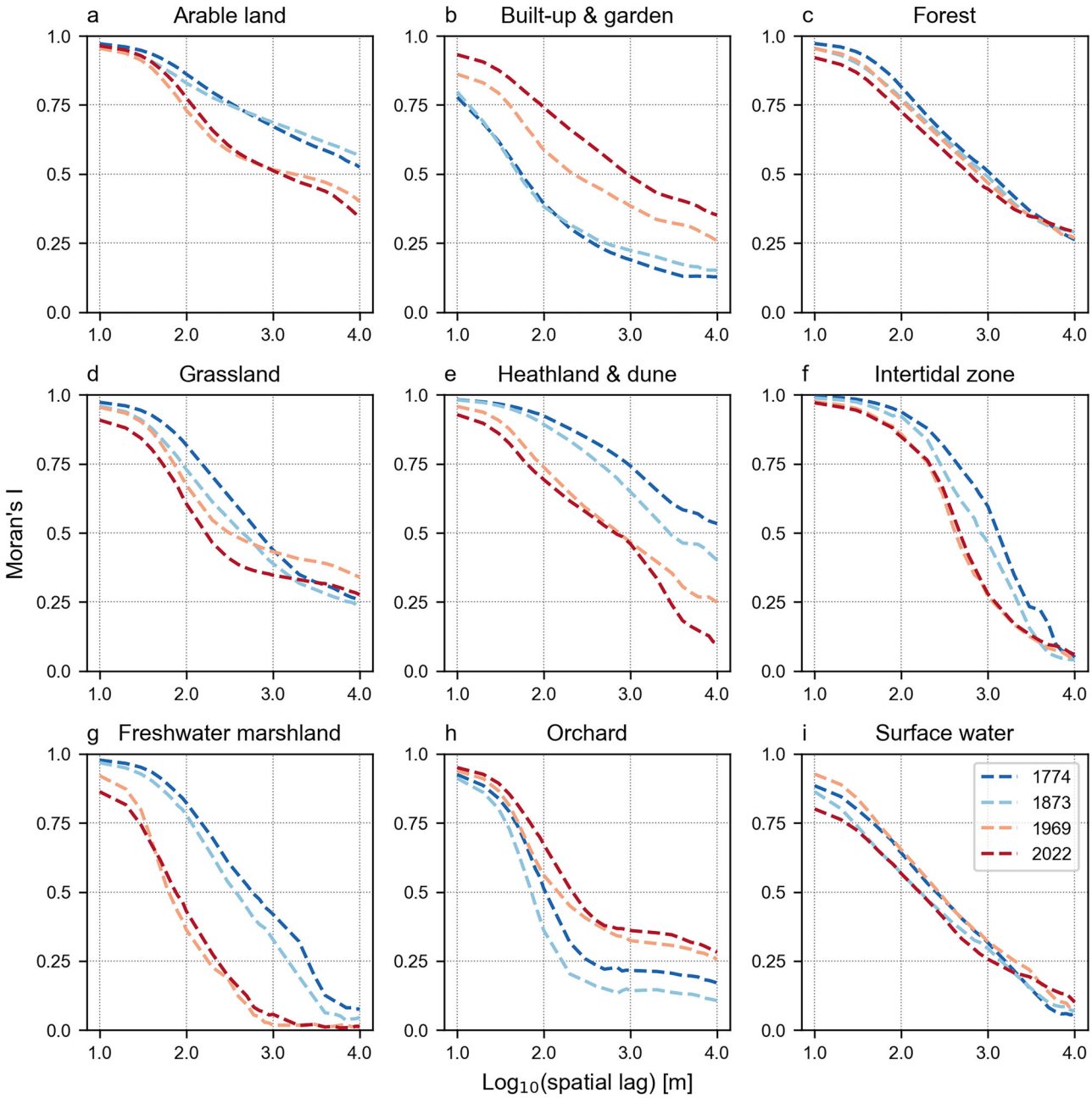

Fig. 5 | Change of spatial autocorrelation of nine land-use classes in northern Belgium, between 1774 and 2022. Global Moran's *I* value (*y*-axis) is calculated as a measure of spatial autocorrelation on 10 × 10 m binary grids of nine land-use classes (**a**–**i**), using an annular kernel with a variable radius or spatial lag (*x*-axis). A value of 1 (*y*-axis) indicates perfect clustering of a land-use class over the evaluated distance (*x*-axis), and declining values indicate decreasing consistency. Negative Moran's *I* values down to −1, which would indicate self-repulsion, were not observed.

The sharp rise of the land-use interspersion level between 1873 and 1969 indicates that landscape transformation culminated in the second time interval. Up to 1873, land-use reflected the soil zonation and delineated distinct landscapes: grasslands in valleys and polders, arable land on sandy loam and silt loam plateaus, heathland & dune and marshland on sand soil. From 1969 onwards, land-use is interspersed to a high degree, in particular by the grassland area that expanded beyond polders and valleys and by progressive urbanization that manifested itself as urban sprawl. As a result, northern Belgium transformed from a mostly rural region with distinct landscapes, to a homogenized peri-urban region. This trajectory could be illustrative for other regions of Europe that show similar growth rates of the urban and peri-urban area (+78%) and the population (+33%) since the mid −1950's[53].

Historical land-use maps, created with GeoAI, are prone to errors and uncertainties that limit the application in research, management and policy[10]. The overall segmentation errors are low in our study, but 6 out of 36 land-use x time combinations have low producer's accuracies. Whereas area estimates are corrected for the bias[54], historical land-use maps subject to spatial analyses are not. Since area proportions of all except one of the aforementioned combinations (built-up & garden in 1874; Table 2) are low, we assume that metrics calculated on all land-use classes are not severely affected. The impact can be higher on autocorrelation, and therefore, the change of fragmentation is evaluated over the whole timespan, including less affected combinations. Another concern are shifting map semantics, meaning that land-use is not depicted in a consistent way by different map series[14,18]. To avoid semantic confusion, classification schemes are

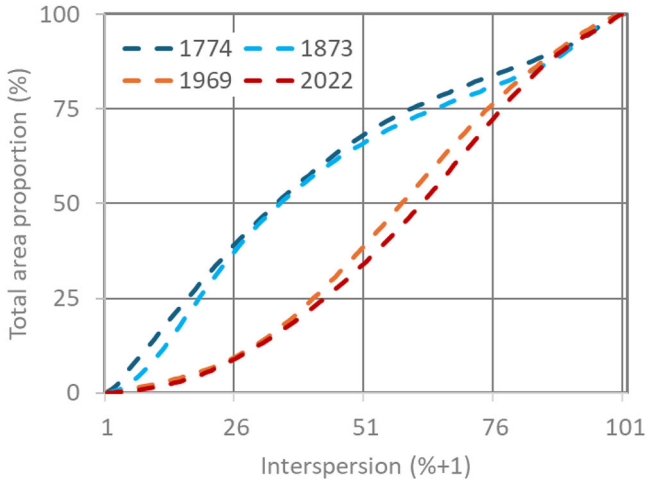

Fig. 6 | The change of the cumulative distribution of the interspersion level in northern Belgium, between 1774 and 2022. The interspersion level, with values from 1 to 101, is the percentage plus one of cells with land-use different from the focal raster cell with 10 × 10 m dimensions, within a circular kernel with a radius of 500 m. The cumulative distribution (*y*-axis) represents the proportion (%) of the total study area with an interspersion level less than or equal to a certain value (*x*-axis).

a prerequisite[14]. We aggregated for this purpose segmentation classes to high-level land-use classes (Supplementary Table S5). However, qualitative changes of land-use over time, e.g., orchards[55], can constrain specific applications of the historical land-use maps. Up to the mid-twentieth century orchards were composed of high-stem trees and also used as grassland[55]. This type of orchard was replaced by plantations of low-stem trees, not suitable for dual use, after World War II. The 1969 map displays both with the same symbol, which complicates the identification of landscapes with heritage values[3], that still contain orchards with high-stem trees.

Here, we demonstrate that GeoAI applied to historical maps can generate high-resolution, area-wide historical land-use maps that open up new opportunities for landscape policy, management, and research. In spite of the high quality of the segmentations, we do not study land-use conversions using an overlay of the consecutive land-use maps, as it would be affected by false land-use change generated by positional errors of the separately created maps[56]. The validation of land-use change classes of the overlay in our case is complicated by the high number of combinations that result from 9 land-use classes on 4 time slices. Furthermore, time intervals up to a century can miss short-lived land-use conversions, e.g., from forest to arable land[57]. In conclusion, the application of GeoAI-generated historical land-use maps is limited less by segmentation accuracy than by changing map semantics, spatial errors, and the interval between consecutive map series.

Methods

Study area and soil typology

Northern Belgium, composed of the administrative Flemish and Brussels capital regions, is a flat or undulating region with an altitude below 290 m above the North Sea level (Fig. 1a), at the southwest side of the North European Plain (Fig. 1b). Topsoils of the North European Plain mainly consist of varying fractions of periglacial Pleistocene eolian sand and silt deposits[58]. As a result, there is a north-south zonation of sand soil, sandy loam soil, and silt loam soil, also present in northern Belgium (Fig. 1c). To determine the association between land-use and soil, the Belgian soil map is reclassified to seven soil groups. This reclassification is based on soil texture and drainage class, which are robust soil properties, shaped by long-term pedogenic processes, that can discern the potential natural vegetation[59]. The potential natural vegetation synthesis map[59] is complemented with polder soils and sand soils of coastal dunes. The Belgian soil map (1:20,000) resulted from the National Soil Survey[60], carried out between 1947 and 1971. Sites classified as disturbed soil, built-up, water, or not surveyed areas, such as military zones, were grouped into a 'not specified' soil group.

The climate of northern Belgium is temperate oceanic, as indicated by averages calculated for 1991–2020[61]. The annual mean temperature was 11.0 °C, and the average daily maximum and minimum temperatures equaled 14.7 °C and 7.3 °C, respectively. On 189.8 days with precipitation per year, an average total precipitation of 837.1 mm was measured. From the North Sea shore in the West towards the eastern border, there is a slight increase in continentality.

At the end of the eighteenth century, the population of northern Belgium was estimated between 1,500,000 and 2,000,000 inhabitants[62]. Census data[63] indicate a population of 3,000,000 in 1873, increasing to 6,500,000 in 1969, and to 8,000,000 in 2022.

Historical and present-day maps

We use the maps of Ferraris that cover the Austrian Netherlands, which belonged to the Habsburg Empire, the first edition of topographical maps of Belgium by Dépôt de la Guerre and the topographical maps of Belgium by the Military Geographical Institute (Supplementary Table S4) for the segmentation of historical land-use. These three historical maps were drawn for military purposes at native scales of 1:11,520, 1:20,000 and 1:25,000, respectively, and are available online as high-quality tiled maps in the Belgian coordinate system (EPSG:31370). The present-day land-use map is composed of the map of land-use in 2022 of the region of Flanders[64], complemented with the capital region of Brussels using the same methodology. The land-use classes of the present-day map of northern Belgium are compiled using 4 database levels, by combination and aggregation of categories from different data levels, to achieve an optimal thematic agreement with the historical maps. The final year of the observations is used to refer to the maps, i.e., 1774, 1873, 1969, and 2022, respectively.

The 1774 map does not completely cover the present-day territory of Belgium and not mapped communities along the present-day border (1.0% of the study area) are excluded from spatial analyses. Areas of the land-use 2022 map assigned to sports and recreation (2.9% of the study area) are also excluded, as they are not discerned on historical maps and presently consist of an unknown mixture of land-use, such as forest, grassland, water, buildings and infrastructure.

The 1774 maps can locally display large distortions, while the surroundings are far less affected[21]. The distortion correction, georeferencing and map tiling for this reason used a high number of 30,000 control points[21], equaling 2.2 control points per km^2. The 1873 and 1969 topographical maps did not need distortion corrections to create tiled maps. At these times, triangulation and leveling techniques were used, based on geodetic bases and reference points marked in the field[65]. Rubbersheeting of the 1774 maps and first-order transformations of the 1873 and 1969 maps, using 2.5 control points per km^2 on a 40 km^2 test area, generated residual Root Mean Square Error (RMSE) values of 34 m, 14 m, and 8 m, respectively. An RMSE below 30 m is a prerequisite to study forest cover changes between 1774 and 2000 in our region[66]. An overlay of 4 instead of 2 maps would require lower RMSE values, as the thematic error increases with the number of included maps[56]. Since the RMSE of the 1774 map exceeds 30 m, we do not analyze land-use conversions using an overlay, but calculate for each time slice proportions of land-use classes in soil groups and vice versa, to quantify the shift of land-use over time in relation to soils.

Land-use segmentation and validation

We use the open source GeoAI software package OrthoSeg version 0.5.0[67] for image segmentation applied to historical maps. The specific legend and drawing of each historical map series require a specific

https://doi.org/10.1038/s41467-026-68594-y

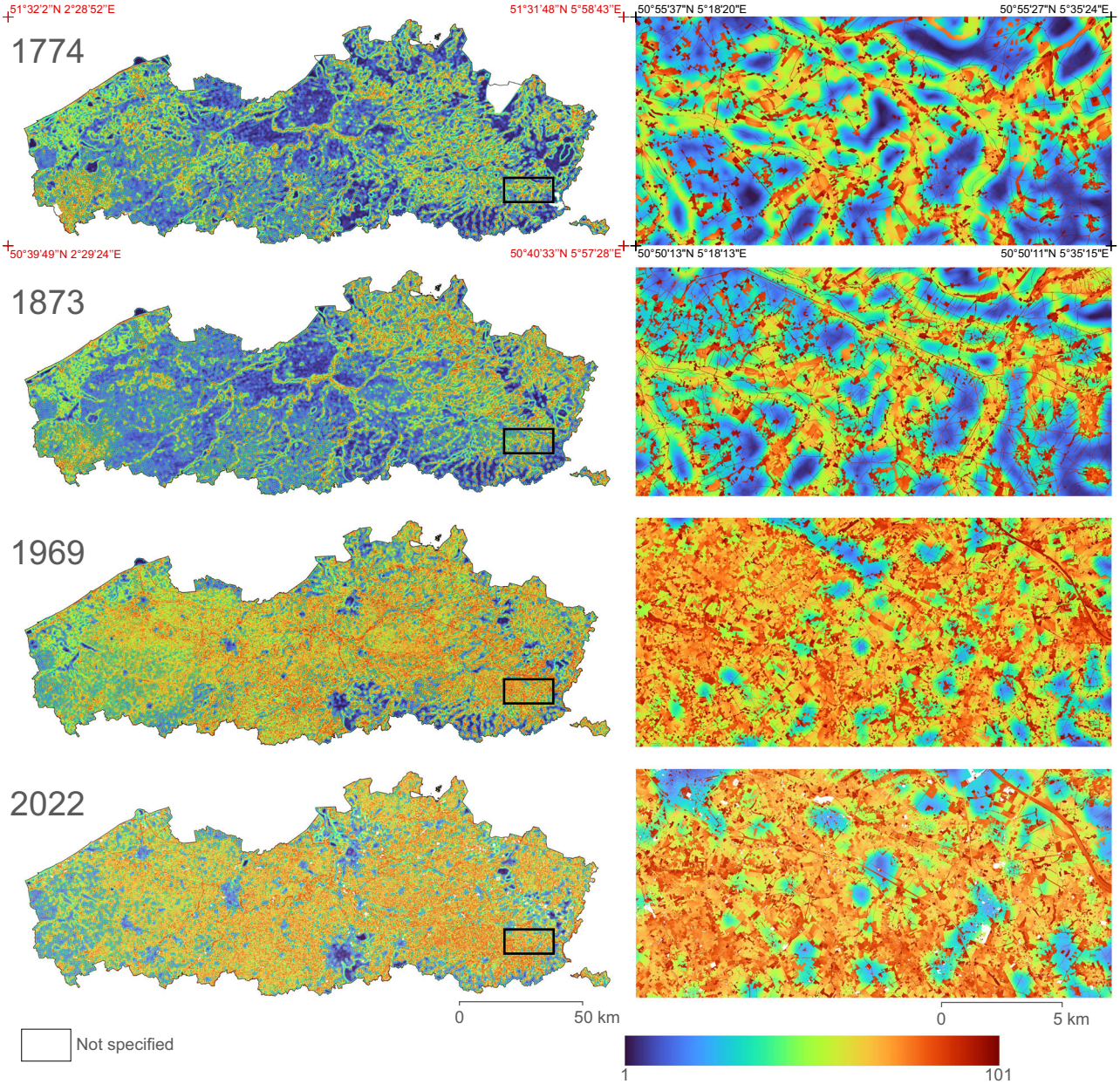

Fig. 7 | Change of the interspersion level in northern Belgium between 1774 and 2022. The interspersion level in northern Belgium (red box in Fig. 1a), with values from 1 to 101 (color legend), is the percentage plus one of cells with land-use different from the focal raster cell with 10 × 10 m dimensions, within a circular kernel with a radius of 500 m. The area of the black box at the transition of silt loam to sand soils (Figs. 1d and 2) is enlarged at the right side.

number of segmentation classes (Supplementary Table S4). The training is based on area-wide manual digitization of segmentation class polygons, in square boxes that measured 256 × 256 m for the 1774 and 1873 maps, and 128 × 128 m for the 1969 map. The prediction runs on downloaded 2048 × 2048 pixel map tiles, with a pixel resolution of 1 m for the 1774 and 1873 maps and 0.5 m for the 1969 map, and with an overlap of 128 pixels for the 1774 and 1873 maps, and 256 pixels for the 1969 map. A first run based on a few and simple training data for the initially discerned segmentation classes is followed by a desktop evaluation of the outcome. Next, additional training boxes are digitized to correct segmentation errors or remove gaps and thus improve the result of the following run. If necessary, additional segmentation classes are discerned and training data of the previous run are adjusted accordingly. This process is repeated until the desktop evaluation was favorable, and comprised 12, 13, and 6 iterations for the 1774, 1873, and 1969 maps, respectively (Supplementary Table S4).

The output of the segmentation is polygon layers for each historical time slice, with 17 (1774), 19 (1873), and 30 (1969) segmentation classes (Supplementary Table S5). These segmentation classes are clustered to 9 common land-use classes and a class with not specified land-use (Supplementary Table S5), which also includes areas of the 2022 map assigned to sports and recreation.

The validation uses area-based error matrices that take into account the selection bias introduced by the stratified sampling of validation points, to calculate the estimated areas and confidence intervals (CI), and the producer's, consumer's and overall accuracies[54] (Supplementary Tables S1–3).

For the validation of the historical land-use maps we select 50–100 points per segmentation class with randomly generated coordinates. The validation points are assigned to the discerned segmentation classes by visual interpretation of the historical map scans, in a QGIS environment. Next, the validation points are clustered to the

9 land-use classes in a similar way as the outcome of the segmentation (Supplementary Table S5).

Spatial analyses

Next, we convert the polygon layers of historical land-use to grids with the same extent and 10 × 10 m cell size as the land-use 2022 map for spatial analyses on land-use classes: the association of land-use classes with soil groups, the spatial autocorrelation of land-use classes, and the interspersion of land-use classes.

We apply the global V-measure, composed of the homogeneity and completeness measures, to assess the degree of spatial association between classes from two categorical maps covering the same area[68], a land-use map with nine classes and a soil map with seven groups in our study. The calculations are performed in Python, using the GDAL and Scikit-Learn packages.

Homogeneity of land-use in soil evaluates the extent to which pixels of a soil group are composed of a single land-use class, with values from 0 to 1. If for each of the seven soil groups the corresponding pixels are composed of only one land-use class, homogeneity of land-use in soil equals 1. If the pixels of the nine land-use classes occur at equal relative frequencies within each of the seven soil groups, homogeneity of land-use in soil equals 0. Completeness of land-use in soil, also with values from 0 to 1, evaluates the extent to which pixels of a land-use class are contained within a single soil group. Completeness of land-use in soil equals 1, if for each of the nine land-use classes all the corresponding pixels are contained within a single soil group. If the pixels of each land-use class are equally divided over the different soil groups, completeness of land-use in soil equals 0. The homogeneity and completeness measures are area-weighted, meaning that more frequently occurring land-use classes or soil groups can have a stronger impact than less frequently occurring ones.

The V-measure V, also comprised between 0 and 1, calculates the harmonic average between the homogeneity h and completeness c measures as follows:

$$V = 2^* \frac{h^* c}{h + c}$$

The four land-use grid layers are also used to evaluate the spatial autocorrelation of land-use classes, i.e., the degree of fragmentation or clustering of land-use. For this purpose, the grid layers are converted to binary maps for each land-use class at each time slice. We calculate the corresponding Moran's I values[69] in Python using the GDAL, Numpy and SciPy packages. Incremental spatial lags, which result in annuli of pixels with a distance between 10 m and 10,000 m from the focal pixel, are used to assess spatial autocorrelation over various distances.

We calculate the interspersion level with the r.neighbors package of grass in QGIS on a focal area with a 500 m radius. The interspersion of a cell is the percentage of cells containing values different from the center cell value, in the circular neighborhood with 500 m radius, plus 1. We select a radius of 500 m since there is a clear change over time of autocorrelation within this distance, for most land-use classes.

Data availability

The tiled historical maps of 1774 can be viewed and accessed at the Geopunt regional geodata portal of Flanders: https://www.vlaanderen.be/datavindplaats/catalogus/ferraris-kaart-kabinetskaart-der-oostenrijkse-nederlanden-en-het-prinsbisdom-luik–1771–1778. Tiled historical topographical maps are online available at the Belgian federal Cartesius geodata portal:Topographical map of 1873: http://www.cartesius.be/arcgis/home/webmap/viewer.html?url=https://wmts.ngi.be/arcgis/rest/services/seamless_carto_default_3857_140/MapServer&lang=en. Topographical map of 1969: http://www.cartesius.be/arcgis/home/webmap/viewer.html?url=https://wmts.ngi.be/arcgis/rest/services/seamless_carto_default_3857_1100/MapServer&lang=en. The maps of segmented historical land-use generated in this study can be viewed and accessed at: https://www.vlaanderen.be/datavindplaats/catalogus/digitalisatie-historisch-landgebruik-en-landgebruiksveranderingen-in-vlaanderen-1778-2022. The land-use map of Flanders in 2022 can be accessed at: https://data.europa.eu/data/datasets/97d565fa-476c-5ea1-8790-b4f88591d611?locale=en.

Code availability

The OrthoSeg open source software package is developed for the segmentation of remote sensing images and maps shared by geoportals[67] and can be accessed at: https://github.com/orthoseg/orthoseg/wiki.

References

1. Le Provost, G. et al. Land-use history impacts functional diversity across multiple trophic groups. *Proc. Natl. Acad. Sci. USA* **117**, 1573–1579 (2020).
2. Foster, D. et al. The importance of land-use legacies to ecology and conservation. *BioScience* **53**, 77–88 (2003).
3. Schulp, C. J. E., Levers, C., Kuemmerle, T., Tieskens, K. F. & Verburg, P. H. Mapping and modelling past and future land use change in Europe's cultural landscapes. *Land Use Policy* **80**, 332–344 (2019).
4. Schirpke, U. et al. Past and future impacts of land-use changes on ecosystem services in Austria. *J. Environ. Manage.* **345**, 118728 (2023).
5. Li, X., Tian, H., Lu, C. & Pan, S. Four-century history of land transformation by humans in the United States (1630–2020). *Earth Syst. Sci. Data* **15**, 1005–1035 (2023).
6. Paprotny, D. & Mengel, M. Population, land use and economic exposure estimates for Europe at 100 m resolution from 1870 to 2020. *Sci. Data* **10**, 372 (2023).
7. Bürgi, M., Östlund, L. & Mladenoff, D. J. Legacy effects of human land use: ecosystems as time-lagged systems. *Ecosystems* **20**, 94–103 (2017).
8. Winkler, K., Fuchs, R., Rounsevell, M. & Herold, M. Global land use changes are four times greater than previously estimated. *Nat. Commun.* **12**, 2501 (2021).
9. Cui, Q. et al. Historical land-use and landscape change in southern Sweden and implications for present and future biodiversity. *Ecol. Evol.* **4**, 3555–3570 (2014).
10. Loran, C., Haegi, S. & Ginzler, C. Comparing historical and contemporary maps—a methodological framework for a cartographic map comparison applied to Swiss maps. *Int. J. Geogr. Inf. Sci.* **32**, 2123–2139 (2018).
11. Lathouwers, E., Segers, Y. & Verstraeten, G. Reconstructing valley landscapes. GIS-analyses of past land use changes in three Flemish river valleys since the late 18th century. *Land Use Policy* **135**, 106960 (2023).
12. Kang, Y., Gao, S. & Roth, R. E. Artificial intelligence studies in cartography: a review and synthesis of methods, applications, and ethics. *Cartogr. Geogr. Inf. Sci.* **51**, 599–630 (2024).
13. Ågren, A. M. & Lin, Y. A fully automated model for land use classification from historical maps using machine learning. *Remote Sens. Appl. Soc. Environ.* **36**, 101349 (2024).
14. Eriksson, S. & Skånes, H. Addressing semantics and historical data heterogeneities in cross-temporal landscape analyses. *Agric. Ecosyst. Environ.* **139**, 516–521 (2010).
15. Martinez, T. et al. Deep learning ancient map segmentation to assess historical landscape changes. *J. Maps* **19**, 2225071 (2023).
16. Suggitt, A. J. et al. Linking climate warming and land conversion to species' range changes across Great Britain. *Nat. Commun.* **14**, 6759 (2023).

17. Ståhl, N. & Weimann, L. Identifying wetland areas in historical maps using deep convolutional neural networks. *Ecol. Inform.* **68**, 101557 (2022).
18. Levin, G., Groom, G. & Svenningsen, S. R. Assessing spatially explicit long-term landscape dynamics based on automated production of land category layers from Danish late nineteenth-century topographic maps in comparison with contemporary maps. *Environ. Monit. Assess.* **197**, 195 (2025).
19. Mäyrä, J., Kivinen, S., Keski-Saari, S., Poikolainen, L. & Kumpula, T. Utilizing historical maps in identification of long-term land use and land cover changes. *Ambio* **52**, 1777–1792 (2023).
20. O'Hara, R., Marwaha, R., Zimmermann, J., Saunders, M. & Green, S. Unleashing the power of old maps: extracting symbology from nineteenth century maps using convolutional neural networks to quantify modern land use on historic wetlands. *Ecol. Indic.* **158**, 111363 (2024).
21. Vervust, S., Boùùaert, M. C., De Baets, B., Van de Weghe, N. & De Maeyer, P. A study of the local geometric accuracy of Count de Ferraris's Carte de cabinet (1770s) using differential distortion analysis. *Cartogr. J.* **55**, 16–35 (2018).
22. O'Rourke, K. H. The European grain invasion, 1870–1913. *J. Econ. Hist.* **57**, 775–801 (1997).
23. Van Dijck, M. & Truyts, T. The agricultural invasion and the political economy of agricultural trade policy in Belgium, 1875–1900. SSRN Scholarly Paper at https://doi.org/10.2139/ssrn.2378740 (2014).
24. Bakker, M. M., Sonneveld, M. P. W., Brookhuis, B. & Kuhlman, T. Trends in soil–land-use relationships in the Netherlands between 1900 and 1990. *Agric. Ecosyst. Environ.* **181**, 134–143 (2013).
25. Mander, Ü, Uuemaa, E., Roosaare, J., Aunap, R. & Antrop, M. Coherence and fragmentation of landscape patterns as characterized by correlograms: a case study of Estonia. *Landsc. Urban Plan.* **94**, 31–37 (2010).
26. Mendels, F. F. Industrialization and population pressure in eighteenth-century flanders. *J. Econ. Hist.* **31**, 269–271 (1971).
27. Ye, Y. et al. Reconstruction of cropland change in European countries using integrated multisource data since AD 1800. *Boreas* **52**, 60–77 (2023).
28. De Moor, M., Shaw-Taylor, L. & Warde, P. Comparing the historical commons of north west Europe. An introduction. In *The Management of Common Land in North West Europe* (eds De Moor, M., Shaw-Taylor, L. & Warde, P.), C. 1500-1850, Vol. 8 15–31 (Brepols Publishers, 2002).
29. Fluet-Chouinard, E. et al. Extensive global wetland loss over the past three centuries. *Nature* **614**, 281–286 (2023).
30. Godet, L. & Thomas, A. Three centuries of land cover changes in the largest French Atlantic wetland provide new insights for wetland conservation. *Appl. Geogr.* **42**, 133–139 (2013).
31. Ryckbosch, W. & Saelens, W. Fuelling the urban economy: a comparative study of energy in the Low Countries, 1600–1850. *Econ. Hist. Rev.* **76**, 221–256 (2023).
32. Tallier, P.-A., Verboven, H., Vandekerkhove, K., Baeté, H. & Verheyen, K. Chapter 3 State forestry in Belgium since the end of the eighteenth century. in *Managing Northern Europe's Fosts: Histories from Three Age of Improvement to the Age of Ecology* (eds Oosthoek, K. J. & Hölzl, R.) 92–129 (Berghahn Books, 2018).
33. Kaplan, J. O., Krumhardt, K. M. & Zimmermann, N. The prehistoric and preindustrial deforestation of Europe. *Quat. Sci. Rev.* **28**, 3016–3034 (2009).
34. Bergès, L. & Dupouey, J.-L. Historical ecology and ancient forests: progress, conservation issues and scientific prospects, with some examples from the French case. *J. Veg. Sci.* **32**, e12846 (2021).
35. Federico, G. The growth of world agricultural production, 1800–1938. In *Research in Economic History* (ed. Field A. J.), Vol. 22 125–181 (Emerald Group Publishing Limited, 2004).
36. Ramankutty, N. et al. Trends in global agricultural land use: implications for environmental health and food security. *Annu. Rev. Plant Biol.* **69**, 789–815 (2018).
37. Swinnen, J. F. M. Agricultural protection growth in Europe, 1870–1969. In *The Political Economy of Agricultural Price Distortions* (ed. Anderson, K.) 141–161 (Cambridge University Press, Cambridge, 2010).
38. Howkins, A. *Reshaping Rural England: A Social History 1850-1925* (Routledge, 2021).
39. Niedertscheider, M., Kuemmerle, T., Müller, D. & Erb, K.-H. Exploring the effects of drastic institutional and socio-economic changes on land system dynamics in Germany between 1883 and 2007. *Glob. Environ. Change* **28**, 98–108 (2014).
40. González de Molina, M. et al. Agricultural output: from crop specialization to livestocking, 1900–2008. in *The Social Metabolism of Spanish Agriculture, 1900–2008: The Mediterranean Way Towards Industrialization* (eds González de Molina, M. et al) 29–68 (Springer International Publishing, 2020).
41. Lohrum, N., Normand, S., Dalgaard, T. & Graversgaard, M. Unveiling the frontiers: historical expansion and modern implications of agricultural land use in Denmark. *J. Environ. Manage.* **359**, 120934 (2024).
42. Moravcova, J., Moravcova, V., Pavlicek, T. & Novakova, N. Land use has changed through the last 200 years in various production areas of South Bohemia. *Land* **11**, 1619 (2022).
43. Bocquier, P. & Costa, R. Which transition comes first? Urban and demographic transitions in Belgium and Sweden. *Demogr. Res.* **33**, 1297–1332 (2015).
44. Angel, S., Parent, S., Civco, D. L. & Blei, A. The persistent decline in urban densities. Lincoln Institute of Land Policy. https://www.lincolninst.edu/publications/working-papers/persistent-decline-urban-densities/ (2010).
45. Mustafa, A. & Teller, J. Self-reinforcing processes governing urban sprawl in Belgium: evidence over six decades. *Sustainability* **12**, 4097 (2020).
46. Poelmans, L. & Van Rompaey, A. Detecting and modelling spatial patterns of urban sprawl in highly fragmented areas: a case study in the Flanders–Brussels region. *Landsc. Urban Plan.* **93**, 10–19 (2009).
47. Thoen, E. & Soens, T. The low countries, 1000-1750. In *Struggling with the Environment: Land Use and Productivity* (eds Thoen, E. & Soens, T.) 221–258 (Brepols Publishers, 2015).
48. Verbeek, T., Boussauw, K. & Pisman, A. Presence and trends of linear sprawl: explaining ribbon development in the north of Belgium. *Landsc. Urban Plan.* **128**, 48–59 (2014).
49. Kuemmerle, T. et al. Hotspots of land use change in Europe. *Environ. Res. Lett.* **11**, 064020 (2016).
50. Rentschler, J. et al. *Rapid Urban Growth in Flood Zones: Global Evidence Since 1985*. Policy Research Working Paper 10014 (World Bank, 2022).
51. Wulf, M., Jahn, U. & Meier, K. Land cover composition determinants in the Uckermark (NE Germany) over a 220-year period. *Reg. Environ. Change* **16**, 1793–1805 (2016).
52. Zgłobicki, W., Gawrysiak, L., Baran-Zgłobicka, B. & Telecka, M. Long-term forest cover changes, within an agricultural region, in relation to environmental variables, Lubelskie province, Eastern Poland. *Environ. Earth Sci.* **75**, 1373 (2016).
53. Ludlow, D. et al. *Urban Sprawl in Europe—The Ignored Challenge* (EEA, 2006).
54. Olofsson, P., Foody, G. M., Stehman, S. V. & Woodcock, C. E. Making better use of accuracy data in land change studies: estimating accuracy and area and quantifying uncertainty using stratified estimation. *Remote Sens. Environ.* **129**, 122–131 (2013).
55. Schönafinger, A., Egarter Vigl, L. & Tasser, E. Spatiotemporal patterns and drivers of orchard meadow loss in South Tyrol. *Italy. Sci. Rep.* **14**, 30812 (2024).

56. Newcomer, J. A. & Szajgin, J. Accumulation of thematic map errors in digital overlay analysis. *Am. Cartogr.* **11**, 58–62 (1984).
57. Verheyen, K., Bossuyt, B., Hermy, M. & Tack, G. The land use history (1278–1990) of a mixed hardwood forest in western Belgium and its relationship with chemical soil characteristics. *J. Biogeogr.* **26**, 1115–1128 (1999).
58. Bertran, P. et al. Revised map of European aeolian deposits derived from soil texture data. *Quat. Sci. Rev.* **266**, 107085 (2021).
59. De Keersmaeker, L. et al. Application of the ancient forest concept to potential natural vegetation mapping in Flanders, a strongly altered landscape in Northern Belgium. *Folia Geobot.* **48**, 137–162 (2013).
60. Dudal, R., Deckers, J., Van Orshoven, J. & Van Ranst, E. Soil survey in Belgium and its applications. In *Soil Resources of Europe* (eds Bullock, P., Jones, R. J. A. & Montanarella, L.) 63–71 (Office for Official Publications of the European Communities, 2005).
61. Royal Meteorological Institute of Belgium (KMI). Klimatologisch jaaroverzichtJaar 2023 https://www.meteo.be/nl/klimaat/klimaat-van-belgie/klimatologisch-overzicht/2023/jaar (2024).
62. Klep, P. M. Population estimates of Belgium, by province (1375-1831). In *Historiens et Populations. Liber Amicorum Étienne Hélin* (ed. Société Belge de Démographie) 458–507 (Academia, 1991).
63. Directorate-General Statistics Belgium (Statbel). Key Figures 2023. https://statbel.fgov.be/en/news/key-figures-2023 (2023).
64. Poelmans, L., Janssen, L. & Hambsch, L. Landgebruik en ruimtebeslag in Vlaanderen, toestand 2022—Onderzoeksportaal. https://www.friscris.be/nl/publications/landgebruik-en-ruimtebeslag-in-vlaanderen-toestand-2022(ab4c67af-a12e-4acf-9346-39df99589565).html (2023).
65. Maeyer, P. D. Base maps in Belgium. *Belg. Rev. Belge Géographie* 165–172 https://doi.org/10.4000/belgeo.13977 (2000).
66. De Clercq, E. M., Clement, L. & De Wulf, R. R. Monte Carlo simulation of false change in the overlay of misregistered forest vector maps. *Landsc. Urban Plan.* **91**, 36–45 (2009).
67. Roggemans, P. orthoseg. Zenodo https://doi.org/10.5281/ZENODO.10340584 (2024).
68. Nowosad, J. & Stepinski, T. F. Spatial association between regionalizations using the information-theoretical V -measure. *Int. J. Geogr. Inf. Sci.* **32**, 2386–2401 (2018).
69. Moran, P. A. P. Notes on continuous stochastic phenomena. *Biometrika* **37**, 17–23 (1950).
70. EuroGeographics. Euro Dem. https://www.mapsforeurope.org/datasets/euro-dem (2023).

Acknowledgements

We thank the National Geographic Institute of Belgium and the Flemish Heritage Agency for the metadata of the historical maps and for their assistance with map interpretation. Timo Ghysels took care of a significant part of the manual digitization of the training locations, and Ingo Buskens validated the segmentation classes. The land-use digitization project was supported by a Flemish Environmental Department grant.

Author contributions

Conceptualization: L.D.K., P.R., and L.P. Methodology: P.R., L.D.K., L.P., F.P., S.T., and T.P. Visualization: L.D.K. and F.P. Funding acquisition: J.V.V. Writing: L.D.K., F.P., L.P., J.V.V., and P.R.

Competing interests

The authors declare no competing interests.

Additional information

Supplementary information The online version contains supplementary material available at https://doi.org/10.1038/s41467-026-68594-y.

Correspondence and requests for materials should be addressed to Luc De Keersmaeker.

Peer review information *Nature Communications* thanks Xiao Huang, Gregor Levin and the other, anonymous, reviewer(s) for their contribution to the peer review of this work. A peer review file is available.